Traffic & Transportation

A Deep Learning Approach for Enhanced Real-Time Prediction of Winter Road Surface Temperatures in High-Altitude Mountain Areas

Meng ZHANG[1], Hua GUO[2], Jing-yang LI[3], Li LI[4], Feng ZHU[5]

Original Scientific Paper
Submitted: 10 Dec 2023
Accepted: 2 Apr 2024

[1] tongjizhangm@163.com, Yunnan Key Laboratory of Digital Communications, Yunnan Yunling Highway Science and Technology Co., Ltd., Yunnan Science Research Institute of Communication Co., Ltd.
[2] 77660291@qq.com, Yunnan Key Laboratory of Digital Communications, Yunnan Yunling Highway Science and Technology Co., Ltd., Yunnan Science Research Institute of Communication Co., Ltd.
[3] ljyebox@foxmail.com, Kunming University of Science and Technology, School of Transportation Engineering
[4] lili@chd.edu.cn, Chang'an University, School of Electronics & Control Engineering
[5] Corresponding author, zhufeng@ntu.edu.sg, Nanyang Technological University, School of Civil and Environmental Engineering

Publisher:
Faculty of Transport and Traffic Sciences, University of Zagreb

ABSTRACT
Low temperatures and icing in winter are significant factors that severely affect highway safety and traffic mobility. To enhance the precision and reliability of real-time winter road surface temperature (RST) prediction, a short-term prediction model is developed that harnesses both feature selection and deep learning. Leveraging meteorological data from a mountain highway in Yunnan, China, the key environmental variables affecting road surface temperature were first extracted using a random forest (RF) model for feature selection. These features were then combined with RST data to construct multiple groups of input variable combinations for the prediction model. A short-term prediction model with a 10-minute update frequency was built using a long short-term memory neural network (LSTM), namely RF-LSTM. The best input variable combination and preset parameters for the prediction model were determined through comparative testing with prevalent machine learning models, and the transferability of the prediction model was verified. The results showed that the best input variable combination for the RF-LSTM prediction model was road surface temperature and air temperature. The model recognised that the short-term RST was affected by long and short-term memory characteristics within a two-hour timeframe. When compared to the RF model, backpropagation (BP) neural network model and the standard LSTM model, the proposed model reduces prediction errors by 59.15%, 31.10% and 20.26%, respectively, while the prediction accuracy is 99.13% within an error margin of ±0.5°C. On the verification dataset, the proposed model maintains its time transferability with an average prediction absolute error of 0.0478. In all, the proposed model not only achieves a higher level of precision in real-time RST predictions but also ensures a more consistent and reliable performance under the challenging conditions of high altitude and mountainous terrain, offering enhanced support for traffic safety and road maintenance decision-making.

KEYWORDS
intelligent transportation system; road surface temperature prediction; long short-term memory model; combination of feature variables; transferability; mountain highway.

1. INTRODUCTION

Winter road icing can deteriorate driving conditions, often resulting in severe traffic accidents and substantial traffic congestion [1]. A key determinant of low-temperature icing is the road surface temperature

(RST). How to accurately predict short-term RST has become a critical issue in the real-time monitoring, warning and risk prevention systems of highway traffic meteorology under icy and snowy weather conditions. While many RST predictions span hourly or daily intervals, short-term RST prediction (in minutes) presents unique challenges. Specifically, short-term predictions are influenced by various non-periodic factors such as localised weather conditions, and the compound temperature of roadbeds and pavements [2]. The effects of these factors are especially prominent in high-altitude mountainous areas, which are characterised by a myriad of climatic conditions, including sharp vertical climatic variations and pronounced local weather differences. Moreover, the complex road conditions and high proportion of structures in mountainous terrains further add to the unpredictability of RST. To address these challenges and enhance prediction accuracy, it is essential to incorporate the specific natural environmental factors of mountain areas and develop a real-time and robust RST prediction model that leverages these factors. It will not only enable early and accurate road icing forecasts but also support the winter implementation of intelligent transportation systems, including traffic meteorology intelligence services, vehicle-road coordination and active vehicle safety control [3].

RST prediction methods in the literature can be primarily divided into three categories: surface energy radiation balance prediction, statistical regression analysis and machine learning algorithms. Surface energy radiation balance prediction is based on thermodynamic principles and road surface radiation energy balance conditions, using mathematical and physical modelling methods to predict RST. Since the 1980s, researchers from various countries, such as Canada [4], France [5] and Finland [6] have been at the forefront of employing this approach for road condition predictions. Over time, significant advancements have been made, such as METRo (model of the environment and temperature of roads) model parameter optimisation [7] and the enhancement of traffic weather observation data [8]. While this method offers a detailed understanding of the impact of external factors on RST, it has its challenges. The associated mathematical and physical models entail multiple parameters that are difficult to obtain, and numerical computation complexity is high. As a result, it is commonly used in RST forecasts for relatively large temporal and spatial scales.

Statistical regression prediction methods are based on historical RST data, using both linear and nonlinear regression models to analyse the correlation between RST and environmental factors such as temperature, total cloud cover and solar radiation [9]. For example, Yin et al. [10] applied multiple linear regression for RST short-term forecasts and achieved a root mean square error of around 1°C for daily prediction. Kršmanc et al. [11] developed an RST prediction model using stepwise linear regression, which outperformed the METRo model when validated using data collected from Slovenian highways. Tang et al. [12] used autoregressive integrated moving average models to predict RST for a 3-hour forecast window and achieved a prediction accuracy of 81.25% within a permissible error margin of ±0.5°C. The majority of statistical regression models boast simplistic structures and are well-suited for datasets of modest sizes, focusing on the prediction of daily maximum/minimum/hourly RST. However, their performance declines when handling RST data characterised by spatio-temporal heterogeneity. Moreover, as the number of variables incorporated into the model increases, maintaining the accuracy, responsiveness and applicability becomes increasingly difficult.

Machine learning algorithms have significant advantages in processing high-dimensional data and modelling complex nonlinear relationships. They have been increasingly applied to RST prediction in recent years. For example, Xu et al. [13] combined dynamic and static predictions in an enhanced backpropagation neural network for RST prediction, which reduces the prediction error of daily temperature change points and can predict the RST for the next 3 hours. Liu et al. [14] introduced gradient boosting into the extreme learning machine, enhancing its performance in RST prediction. Wang et al. [15] used composite features to characterise the interactions and temporal changes in RST features, improving the performance of the random forest RST prediction model. Qiu et al. [16] utilised association rule mining algorithms to analyse the correlation between meteorological factors and RST. Long short-term memory (LSTM) models, recognised for their capacity to simultaneously learn short-term and long-term behavioural patterns in time series data [17–19], have been deployed effectively for RST prediction. For example, Tabrizi et al. [20] integrated convolutional neural networks (CNN) and LSTM models for hourly RST prediction, highlighting LSTM's proficiency in tracking temperature changes. Dai et al. [21] explored the cumulative effects of various external factors on winter highways and the periodicity of RST and proposed an RST hourly prediction model with an accuracy of 90% within an error margin of ±1°C. In all, existing machine learning-based RST prediction methods present several challenges. (1) Most studies focus on hourly or daily maximum/minimum RST predictions, with few targeting short-term predictions in minute intervals; (2) while some studies use correlation analysis to select influential parameters for RST, many rely solely on univariate time series RST. There is a notable gap in studies that quantitatively analyse the impact of multi-dimensional input features and

their combinations; (3) most studies evaluate the predictive performance of the model with a testing set, without examining the transferability of the model through a validation set, and there are few studies comparing the performance of different RST machine learning algorithms.

To address the above challenges, this study constructs an RF-LSTM model tailored for short-term RST predictions, set at a 10-minute interval. The RF algorithm aids in pinpointing significant features that have a notable impact on RST. These important parameters, arranged by their significance, are then merged with RAS to serve as candidate inputs for the LSTM model. By evaluating the predictive performance of different feature combinations and selecting the optimal input parameters, the most efficient prediction model is obtained. The time transferability of the model is further validated with a separate validation dataset. This study provides references for determining pertinent input features that affect winter road surface temperatures and paves the way for developing more effective short-term prediction models for RST.

2. DATA

In this section, a minute-by-minute dataset of highway traffic meteorology is introduced for training the machine learning-based RST prediction models. The dataset was collected from a high-altitude mountainous highway in Yunnan province, China; it serves as a typical case study for short-term RST prediction and early icing warning applications.

2.1 Data source

The data for this study were collected from the Niujia Gou Bridge on the Ma Zhao Expressway in the Wumeng Mountain area of Yunnan Province in China. Elevated at 217 meters above the valley bottom, the bridge deck is particularly prone to icing in winter due to various environmental factors such as steep slopes, bridge decks, headwinds and low temperatures. Road icing conditions have recurrently led to traffic accidents and disruptions. The traffic meteorological station located at Niujia Gou Road, as shown in *Figure 1*, is equipped with automatic sensing devices for monitoring various traffic and meteorological conditions. The key devices installed at this station include the Vaisala DSC111 Road Surface Condition Sensor, Vaisala WXT520 Weather Six-Element Sensor and Vaisala PWD22 Visibility Sensor, which collectively gather crucial data for our study. In this study, traffic meteorological data were collected from January 2020, with an interval of 1 minute. The collected data include nine meteorological environmental features (air temperature, humidity, air pressure, wind speed, wind direction, visibility, precipitation, water film, ice layer and snow layer thickness), along with three road surface state features (RST, wet coefficient and road surface condition). To assess the accuracy and transferability of the model, we employed a 5-fold cross-validation approach. This method ensures the reliability of our analytical results by rigorously testing the model across multiple subsets of the data.

Figure 1 – Roadside traffic meteorological station located at Ma Zhao Expressway, Yunnan, China

2.2 Data preprocessing

During the data acquisition phase from the traffic meteorological station, various uncontrollable factors result in anomalies in the RST data such as missing data, noise and outliers. Therefore, preprocessing of the

obtained RST dataset is essential. Firstly, *Equation 1* is used to transform the 1-minute traffic meteorological element data into samples at 10-minute intervals, which helps in reducing the impact of noise and outliers on the samples;

$$x_{10\min} = \frac{(x_i + x_{i+2} + \cdots + x_{i+10})}{10} \tag{1}$$

where x_i represents the meteorological data collected by the station every minute (i=0,1,2…,*M*), *M* is the total number of samples; ; $x_{10\min}$ denotes the 10-minute moving average of the meteorological data. The smoothed data effectively eliminate abrupt abnormal values in RST data at 1-minute intervals, while preserving the temperature change pattern. Given that multiple sensors are used for data collection at the traffic meteorological station, there may be dimensional differences in measurements. Therefore, the data processed from *Equation 1* further undergoes Z-score normalisation:

$$x^*_{10\min} = \frac{x_{10\min} - u}{\sigma} \tag{2}$$

where u represents the arithmetic mean of $x_{10\min}$, σ represents the standard deviation of $x_{10\min}$, and $x^*_{10\min}$ represents the normalised value

3. MODEL

In this section, the framework of the RF-LSTM model for RST prediction is proposed. Specifically, this section introduces the algorithm of feature selection and combination for the RST prediction model input, details the LSTM model structure, presents the sliding time window-based mathematical representation of the RST prediction model and outlines the evaluation metrics used to measure the performance of the model.

3.1 Model framework

The framework designed for the short-term RST prediction model, tailored for highways in high-altitude mountainous areas, is presented in *Figure 2*. The framework uses the RF algorithm to rank the importance of external meteorological environmental features and road surface state features that may affect RST, and subsequently select the candidate features with significant impact. These candidate features are then combined with RST to serve as model inputs. The best-performing combination of features is selected based on the prediction performance. An LSTM-based RST prediction model is built and trained to determine the optimal model parameters. The structures and functions of the framework are described in detail below.

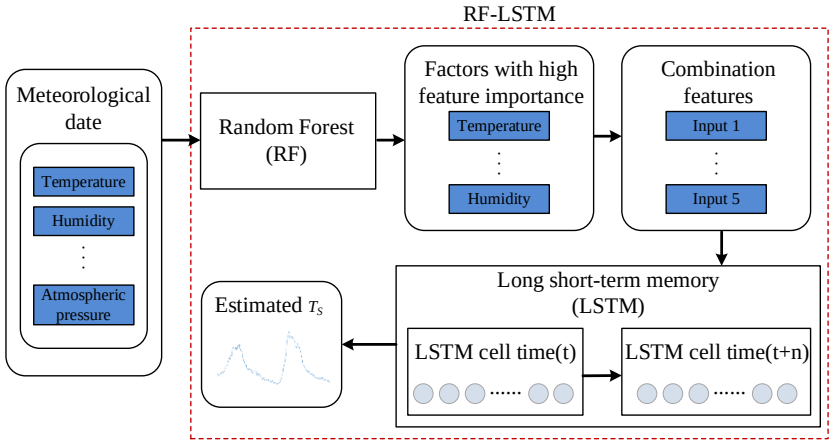

Figure 2 – Framework of RST prediction based on the RF-LSTM model

3.2 Feature selection and combination

RF is an ensemble learning algorithm that incorporates randomness into decision tree training [22–23], which can identify important features from a large amount of sample data. The basic principle of RF feature selection is the strategy of adding noise to a particular feature. If the accuracy of the model on out-of-bag data drops significantly due to this noise, it indicates that the feature plays a pivotal role in the model and is of high importance. The screening process is as follows:

— Step 1: a resampled set of samples $b = 1, 2, \ldots, B$ is obtained, where B is the total number of training samples;
— Step 2: with $b = 1$, multiple samples are randomly selected from the training samples to create a regression tree T_b, and the out-of-bag data is labelled as L_b^{oob};
— Step 3: T_b is used to regressively predict the L_b^{oob} data on the out-of-bag data, and the out-of-bag error is calculated and denoted as $Error_{oob1}$;
— Step 4: for feature $X_j (j = 0,1,2 \ldots, P)$, where P is the total number of feature variables, the value of feature X_j in L_b^{oob} is perturbed, and the perturbed dataset is denoted as L_{bj}^{oob}. T_b is then used to regressively predict the L_{bj}^{oob} data, and the out-of-bag error is calculated and denoted as $Error_{oob2}$;
— Step 5: for $b = 2, \ldots, B$, steps 2 – 4 are repeated;
— Step 6: the importance of feature X_j is calculated $\overline{D_j}$.

$$\overline{D_j} = \frac{\sum_{i=1}^{B} (Error_{oob1} - Error_{oob2})}{B} \tag{3}$$

Following the analysis, *Figure 3* presents the importance ranking of meteorological environmental features and road surface state features as collected by the meteorological station. Features with importance greater than 2% (namely, temperature, air pressure, wind speed, humidity and wind direction) are selected as external environmental feature variables that characterise the impact on RST. Air pressure ranks as the second most important, indicating that the altitude and terrain topography present a considerable impact on RST on the mountainous highway.

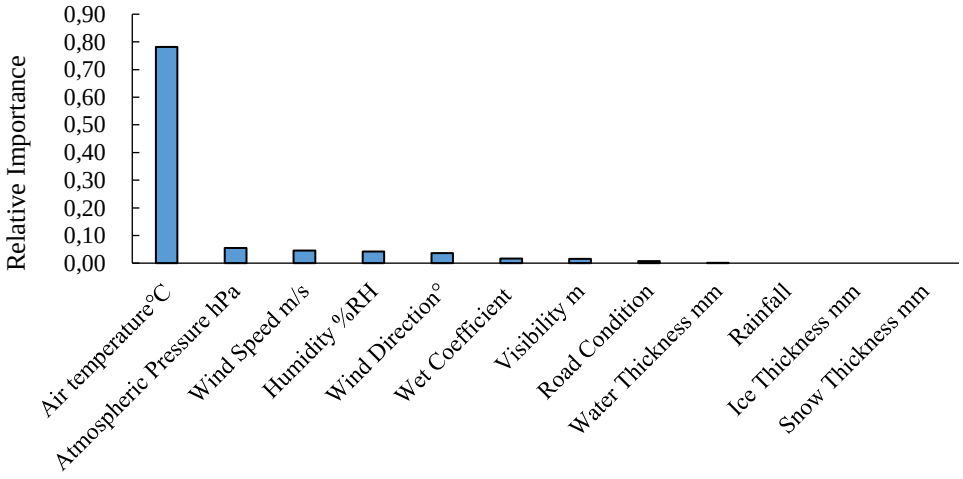

Figure 3 – Importance order of feature variables

According to the importance ranking of the five candidate features, five sets of candidate input feature combinations are constructed:
1) RST + temperature (variable combination 1),
2) RST + temperature + air pressure (variable combination 2),
3) RST + temperature + air pressure + wind speed (variable combination 3),
4) RST + temperature + air pressure + wind speed + humidity (variable combination 4) and
5) RST+ temperature + air pressure + wind speed + humidity + wind direction (variable combination 5). Each of these combinations serves as the feature input (vectors $\boldsymbol{X}$) for the LSTM model.

3.3 RST short-time prediction model

Since RST is influenced by the cumulative effect of past RST data, it is necessary to consider the impact of historical RST data on the current RST when predicting RST in real-time. The LSTM model, a deep learning algorithm designed for sequential data, aptly addresses this need. It overcomes the long-term dependency limitation inherent to recurrent neural networks (RNN), offering enhanced proficiency in time series data prediction. The structure of the LSTM model is depicted in *Figure 4*, where x_t represents the input feature at time t, s_t represents the hidden layer state at time t, and c_t represents the cell state.

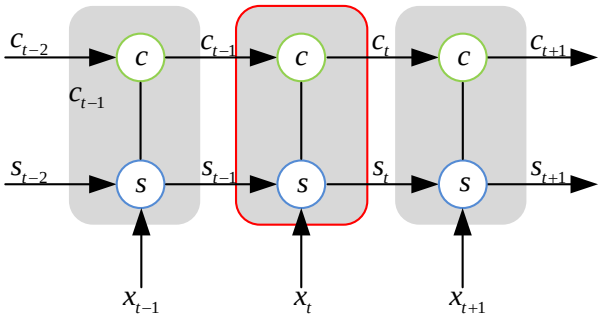

Figure 4 – Structure of the LSTM model

In the model learning process, LSTM modulates the cell state through the integration of input gates, forget gates and output gates. The process is detailed as follows: first, the forget gate determines the information to be discarded from the old cell state according to *Equation 4*; the input gate determines the proportion of new information to be updated into the old cell state as per *Equation 5*. Meanwhile, *Equation 7* is used to determine the data information that needs to be updated; the new cell state is composed of the information retained after passing through the forget gate and the updated new information from the input gate, which is calculated by *Equation 8*; finally, LSTM outputs h_t which is determined by the output gate and the new cell state, calculated by *Equation 9*.

$$f_t = \sigma(W_f \cdot [h_{(t-1)}, x_t] + b_f) \tag{4}$$

$$i_t = \sigma(W_i \cdot [h_{(t-1)}, x_t] + b_i) \tag{5}$$

$$o_t = \sigma(W_o \cdot [h_{(t-1)}, x_t] + b_o) \tag{6}$$

$$C_t' = \tanh(W_c \cdot [h_{(t-1)}, x_t] + b_c) \tag{7}$$

$$C_t = f_t \cdot C_{t-1} + i_t \cdot C_t' \tag{8}$$

$$h_t = o_t \cdot \tanh(C_t) \tag{9}$$

f_t denotes the forget gate, i_t denotes the input gate, o_t denotes the output gate, C_t denotes the cell state and h_t denotes the hidden layer output.

Due to the dynamic and correlative short-term changes in the RST temporal data on mountainous roads, and the lag effect of external environmental factors such as temperature, humidity and air pressure that affect the process of RST through interactions with road surface materials and structures, the RST y_t at any given time t is not solely influenced by the concurrent feature variable $\boldsymbol{X}_t$ (composed of feature vectors such as temperature, air pressure, wind speed, humidity and wind direction), but also by the crucial feature variables of the previous k moments, with the influence weakening as the time step k increases. To accommodate this, the proposed RST prediction model adopts the sliding time window method, as presented in *Figure 5*.

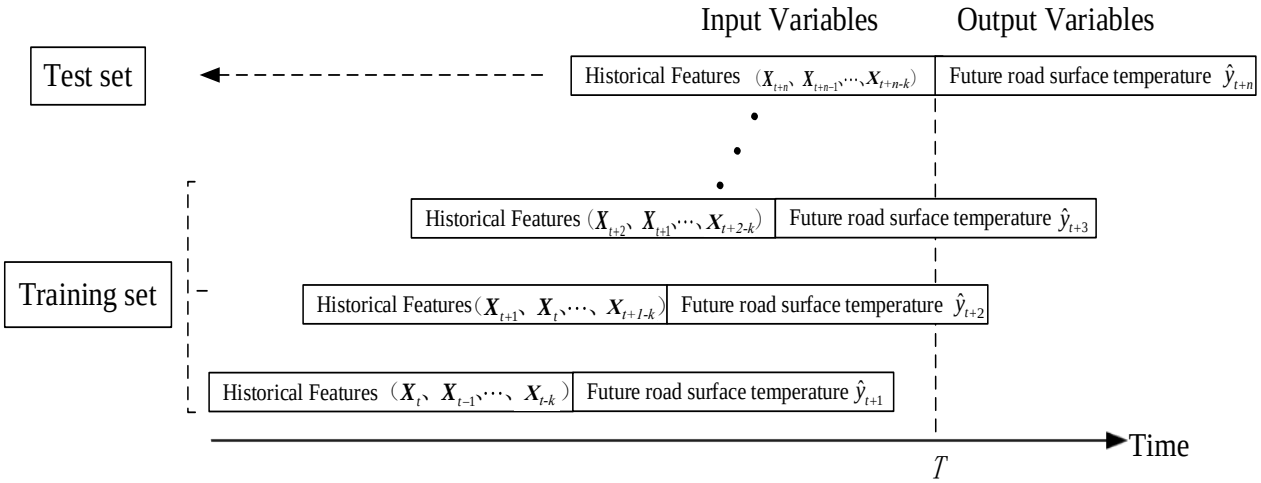

Figure 5 – Sliding time window

Specifically, data from each time interval are segmented into separate windows with a step size of 10 minutes. The model utilises historical features from the previous segment to predict the RST of the next 10 minutes and continues this process iteratively. Consequently, the input vector $\boldsymbol{MI}$ of the LSTM model at time t consists of the RST values of the previous k moments ($y_t, y_{t-1},\ldots, y_{t-k}$) and the corresponding feature vectors ($\boldsymbol{X_t}, \boldsymbol{X_{t-1}},\ldots, \boldsymbol{X_{t-k}}$). The output is the predicted RST value $\hat{y}_{t+1}$ of the next 10 minutes (i.e. time $t+1$). The mathematical representation for the input and output of the LSTM model is:

$$\hat{y}_{t+1} = f(\boldsymbol{MI}) \tag{10}$$

where $f(\cdot)$ represents the non-linear approximation function of the LSTM model.

3.4 Evaluation indicators

To select the best-performing combination of input feature variables and model parameters, and to evaluate the transferability of the model, we employed mean absolute error (MAE), mean absolute percentage error (MAPE), mean squared error (MSE) and root mean squared error (RMSE) as evaluation metrics. Specifically, MAE intuitively reflects the magnitude of the absolute error between predicted and actual values, MAPE indicates the reliability and accuracy of the prediction model, while MSE and RMSE capture the degree of the distribution spread of the prediction errors. A smaller value across MAE, MAPE, MSE and RMSE indicates better predictive performance of the model.

$$MAE = \frac{\sum_{i=1}^{N} |y_i - \hat{y}_i|}{N} \tag{11}$$

$$MAPE = \frac{\sum_{i=1}^{N} \left| \frac{(y_i - \hat{y}_i)}{y_i} \right|}{N} \cdot 100\% \tag{12}$$

$$MSE = \frac{\sum_{i=1}^{N} (y_i - \hat{y}_i)^2}{N} \tag{13}$$

$$RMSE = \sqrt{\frac{\sum_{i=1}^{N} (y_i - \hat{y}_i)^2}{N}} \tag{14}$$

4. RESULTS

In the process of model training, the selection of model hyperparameters and the optimisation of model structure are equally important. This section is dedicated to the model structure optimisation and hyperparameter selection of the proposed RF-LSTM. It also includes the evaluation of the prediction performance of RF-LSTM in comparison to three other widely used machine learning models: RF, LSTM and BP neural network.

4.1 Model parameter selection

The RF-LSTM model was built using the Keras framework with the 5 candidate feature variable combinations determined in Section 2.2 as model inputs. The mean absolute error (MAE) was used as the loss function and Adam was chosen as the model optimiser. The model was trained on the training dataset and validated using the test dataset. Taking input variable combination 1 as an example while holding other hyperparameters constant, the number of LSTM hidden layers was varied within the range {1, 2, 3}. The results, shown in *Table 1*, revealed that the 3-layer LSTM network had the poorest prediction performance, likely due to overfitting. Meanwhile, the single-layer network had a roughly 3% lower MAE compared to the double-layer network and demonstrated a faster training speed. Therefore, this study employed an LSTM model with a single layer of hidden neurons. A search was carried out for time steps k within the set {2, 4, 6, 8, 10, 12, 14, 16}. The best time step k was selected based on the minimum MAE. The prediction performance shown in *Table 2* identified k as 12, which corresponds to predicting future 10-minute output using past 2-hour data.

The determination of other hyperparameters followed similar approaches. Finally, a three-layer neural network consisting of an input layer, an LSTM layer with 20 neurons and an output layer was constructed. The learning rate was set to 1×10^{-3}, the time step k was set to 12, the batch size was set to 128 per epoch, the maximum number of epochs was set to 150, and the model loss stabilised at around 0.03.

Table 1 – Prediction results of the LSTM models with different number of hidden layers

LSTM layers	MSE	RMSE	MAE	MAPE(%)
1 layer	0.0015	0.0397	0.0309	10.6286
2 layer	0.0016	0.0406	0.0319	10.7234
3 layer	0.0025	0.0508	0.0420	12.1654

Table 2 – Prediction results of the models with different numbers of time lags

Time steps	2	4	6	8	10	12	14	16
MSE	0.0021	0.0018	0.0017	0.0019	0.0015	0.0014	0.0015	0.0015
RMSE	0.0463	0.0427	0.0418	0.0442	0.0391	0.0383	0.0392	0.0397
MAE	0.0371	0.0335	0.0329	0.0357	0.0305	0.0294	0.0301	0.0306
MARE (%)	12.4828	11.0255	11.0415	11.2058	10.2850	10.1030	10.3449	10.8402

The predictive outcomes of the RST with 5 different input feature variable combinations are shown in *Table 3*. Among them, the prediction for input variable combination 4 was the worst, while the best prediction was obtained using RST and temperature as model inputs (input variable combination 1), followed by RST, temperature, and atmospheric pressure combination (input variable combination 2). It suggests that the complexity of the LSTM model increases with the number of input variables, leading to a higher likelihood of overfitting and the subsequent decline in prediction accuracy.

Table 3 – Prediction results of the models with different input variable combinations

Input variable combinations	MSE	RMSE	MAE	MAPE(%)
1	0.0015	0.0397	0.0299	10.3584
2	0.0022	0.0472	0.0360	11.9511
3	0.0024	0.0495	0.0349	12.3670
4	0.0025	0.0508	0.0373	12.6454
5	0.0022	0.0478	0.0365	12.5079

4.2 Prediction accuracy analysis

To offer a comprehensive evaluation of the RST predictive performance of the RF-LSTM model, the BP neural network model [24], RF model and standard LSTM model were used as baseline models for comparison. BP and RF models used historical 2-hour RST data as input data, while the standard LSTM model used 12 candidate features as input. After multiple trial tuning, the optimal parameter configuration for the BP model was set with five neurons in the input layer, ten neurons in the hidden layer, batch processing amount of 128, 300 iterations, Adam optimiser for optimisation, Relu as the activation function and mean squared error as the loss function. The RF model was constructed using the Sklearn library and used the Bagging method integration and CART regression tree as the core function. Optimal parameter configuration was achieved with 300 regression trees and a maximum depth of 9. The parameters for the standard LSTM model were the same as the RF-LSTM model.

Figure 6 illustrates the convergence trends of MAE for four predictive models. As observed, the RF-LSTM hybrid model exhibits a superior convergence profile, achieving the lowest MAE rapidly within the initial iterations and maintaining this lead throughout the training process. The LSTM model closely follows, suggesting the effectiveness of memory units in capturing temporal dependencies for the task at hand. Both the RF and BP models demonstrate similar convergence patterns, albeit with slightly higher MAE values. The convergence curves of all models stabilise after approximately 1,000 iterations, indicating a plateau in the learning where additional iterations cease to yield significant improvements in predictive accuracy.

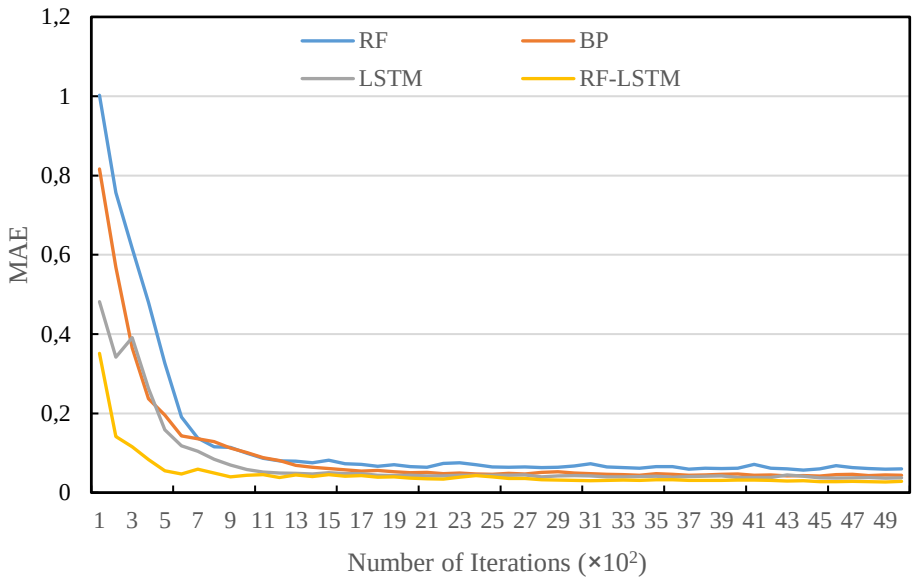

Figure 6 – Convergence trends of MAE for different models

The results of the predicted performance of the four RST prediction models are shown in *Table 4*. Overall, the RF-LSTM outperformed the rest, followed by the LSTM, BP and RF model in terms of predictive accuracy and precision. Specifically, the predicted mean MAE and MAPE of the RF-LSTM model were 0.028834 and 10.5146%, respectively. Compared with the RF model, which had mean MAE and MAPE values of 0.060898 and 16.76245%, the RF-LSTM model improved the mean accuracy by approximately 52.68% (in MAE) and enhanced the predictive precision by about 37.32% (in MAPE). The RF model, despite showing competence on the training dataset, was less effective on the testing dataset. In contrast to the other supervised learning algorithms, the RF model, as an ensemble learning approach, was more susceptible to overfitting and exhibited the weakest generalisation ability.

The time series curves of the RST predicted and actual values across the four models are shown in *Figure 7*. It is seen that RST presents complex nonlinear time-varying characteristics, with notable differences in performance among different models.

1) In the winter season with temperatures ranging from 0 to 2.5°C and during periods of frequent RST fluctuations, the RF model demonstrates significant deviation between the predicted and actual values.
2) The predictions of the BP model are generally more stable than the RF model's predictions. However, within the temperature range of 0 – 2.5°C and the high-temperature peak period of RST, the prediction error remains pronounced. This could be attributed to the limited samples at these temperature extremes, causing the BP model to be prone to overfitting.
3) The predicted RST values from both the LSTM model and RF-LSTM model generally follow the pattern of actual data, with the RS-LSTM model showing superior performance. The LSTM model exhibited a "jump" in the predicted values around the 300th testing data point, resulting in a considerable prediction error. This could be due to the LSTM model incorporating all the features as input, leading to sudden changes in input variables triggered by sudden weather events such as rapid rise in humidity from heavy rain or surge in wind speed from gusts, thereby reducing the predictive performance.
4) Compared to the standard LSTM model that utilises all the feature variables, the RF-LSTM model achieved a reduction of 44.4%, 23.6%, 24.3% and 16.3% in terms of MSE, RMSE, MAE and MAPE, respectively. This indicates that with an optimised combination of input variables based on crucial feature extraction, the RF-LSTM model possesses stronger generalisation capability and superior predictive performance.

Table 4 – Prediction results of four models

Models	Fold	MSE	RMSE	MAE	MAPE(%)
RF	1	0.01539	0.12405	0.05794	17.57103
	2	0.01327	0.11519	0.06243	17.68812
	3	0.01517	0.12316	0.06325	16.41573
	4	0.01214	0.11018	0.04655	16.61939
	5	0.01179	0.10858	0.07432	15.51797
	mean	0.013552	0.11623	0.060898	16.76245
	Fold	MSE	RMSE	MAE	MAPE(%)
BP	1	0.00243	0.04929	0.02853	15.31311
	2	0.00435	0.06595	0.03627	13.65691
	3	0.0033	0.05744	0.05535	12.97443
	4	0.00225	0.04743	0.04565	12.14034
	5	0.00226	0.04753	0.05599	14.58002
	mean	0.002918	0.05353	0.04435	13.73296
	Fold	MSE	RMSE	MAE	MAPE(%)
LSTM	1	0.00372	0.06099	0.03145	11.93011
	2	0.00367	0.06058	0.05066	12.46415
	3	0.00365	0.06041	0.02912	12.77099
	4	0.00213	0.04615	0.03382	13.29561
	5	0.00345	0.05873	0.03989	12.06485
	mean	0.00332	0.05737	0.03698	12.50514
	Fold	MSE	RMSE	MAE	MAPE(%)
RF-LSTM	1	0.00121	0.034785	0.02841	10.20143
	2	0.00169	0.04110	0.03022	9.79981
	3	0.00183	0.04277	0.02515	10.83917
	4	0.00155	0.03937	0.02748	11.51501
	5	0.0013	0.03605	0.03291	10.21756
	mean	0.00151	0.03881	0.02883	10.51467

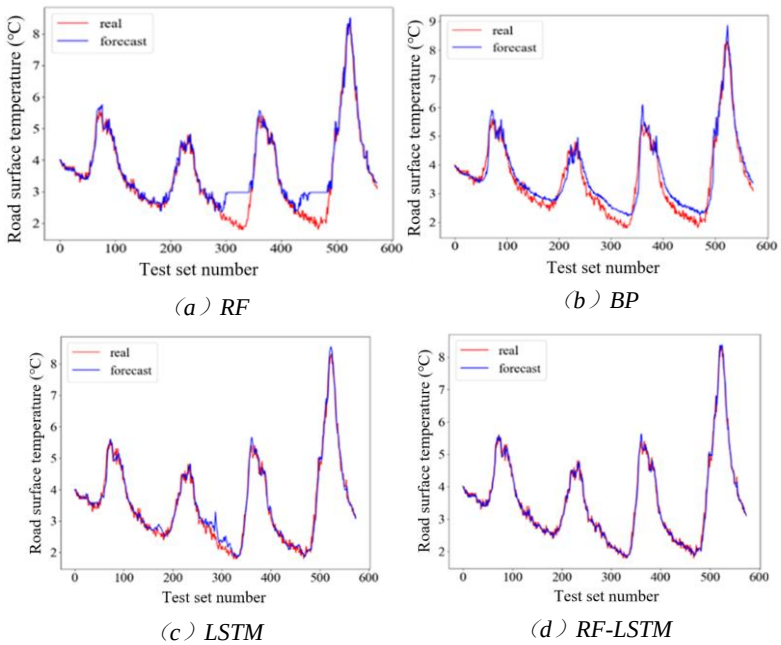

（a）*RF*　（b）*BP*

（c）*LSTM*　（d）*RF-LSTM*

Figure 7 – Prediction results with different models

4.3 Prediction error

By analysing the prediction error and accuracy of the RF-LSTM model, as shown in *Table 4*, its accuracy and practicability are validated to be within the allowable error range. Notably, the RF-LSTM model achieved an MAE of 0.0485 on the training data, which translates to 0.184°C for RST, while for the testing data, the RF-LSTM model achieved an MAE of 0.0299, equivalent to 0.114°C for RST. The model exhibited small prediction errors and high prediction accuracy. The RST prediction error curve is illustrated in *Figure 8*. Overall, the RF-LSTM model's prediction error lies within the ±0.5°C control margin, confirming the accuracy of its predictions.

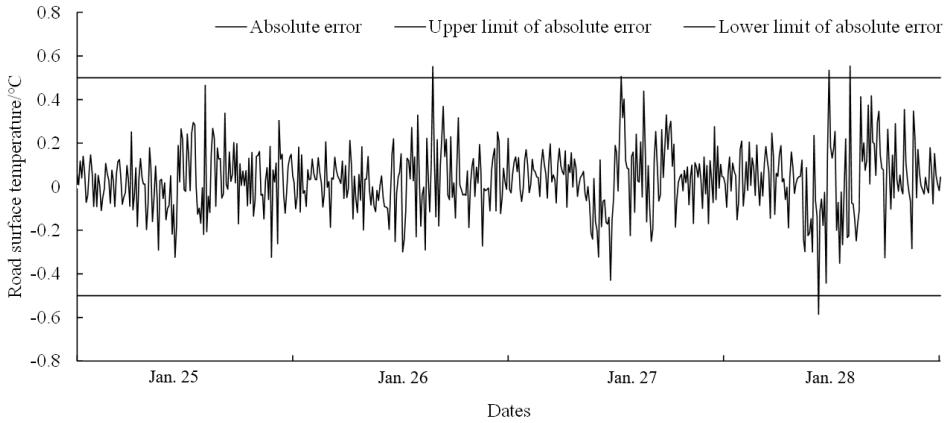

Figure 8 – Absolute error of 0.5°c control line for RST prediction

The prediction accuracy of the RF-LSTM model across different allowable error ranges is presented in *Table 5*. Within the ±0.5℃ allowable error range, the prediction accuracy of the RF-LSTM model reached 99.13%. This level of precision is particularly promising when compared with the allowable error of ±2℃ on general road sections. Especially, the RF-LSTM model meets the requirement of ±0.5℃ allowable error on bridge sections and exhibits higher prediction accuracy. The superior performance is achieved by optimising the combination of RF and feature variables to filter out noise caused by sudden changes and combining the characteristics of the LSTM model to update weights and thresholds in real-time. Consequently, the RF-LSTM model stands out for its high prediction accuracy and strong robustness. It shows good engineering practicality for short-term forecasting and early warning of road surface icing in winter.

Table 5 – Prediction accuracy of the RF-LSTM model for different allowable error ranges

Allowable error range/(℃)	±0.5	±1	±2
Prediction accuracy/(%)	99.13	100	100

4.4 Model transferability

The trained and tested RF-LSTM model was further validated using a separate dataset to evaluate its predictive accuracy. The distribution of the measured and predicted values of the four models along the 45-degree reference line is shown in *Figure 9*. It can be observed that the predicted and measured values of the RF-LSTM model are clustered around the 45-degree line, which indicates a significant correlation between the two. Compared to the test set results in *Table 2*, although the prediction accuracy of the RF-LSTM model decreased slightly, with an MAE of only 0.0478 (equivalent to RST of 0.18°C) and the MAPE of 22.43%, the model still exhibits high prediction accuracy, stability and satisfactory performance within the allowable error range in engineering practice.

Regarding the baseline models, the standard RF model had the largest dispersion between the predicted and measured values, with an MAE of 0.0890 (equivalent to RST of 0.33°C), and the MAPE of 31.53%, which increased by nearly 15% compared to the test set. The predicted values and measured values of the BP model were more widely dispersed in the low-temperature and high-temperature intervals, and the difference between them was significant. Its MAPE increased from 14.18% in the test set to 31.17%, signifying a significant drop in prediction accuracy. The clustering degree of the LSTM model's predicted values and measured values was weakened in the low-temperature interval during winter, and the value predicted in the high-temperature

interval of 6 – 14°C fluctuated significantly. Its MAE was 0.0561, and the MAPE increased from 12.38% in the test set to 27.72%. The decline in performance could be attributed to the inclusion of all 12 input feature variables of the original data. The high-dimensional input variable combination made the LSTM model more complex and prone to overfitting. Consequently, its transferability was found to be mediocre.

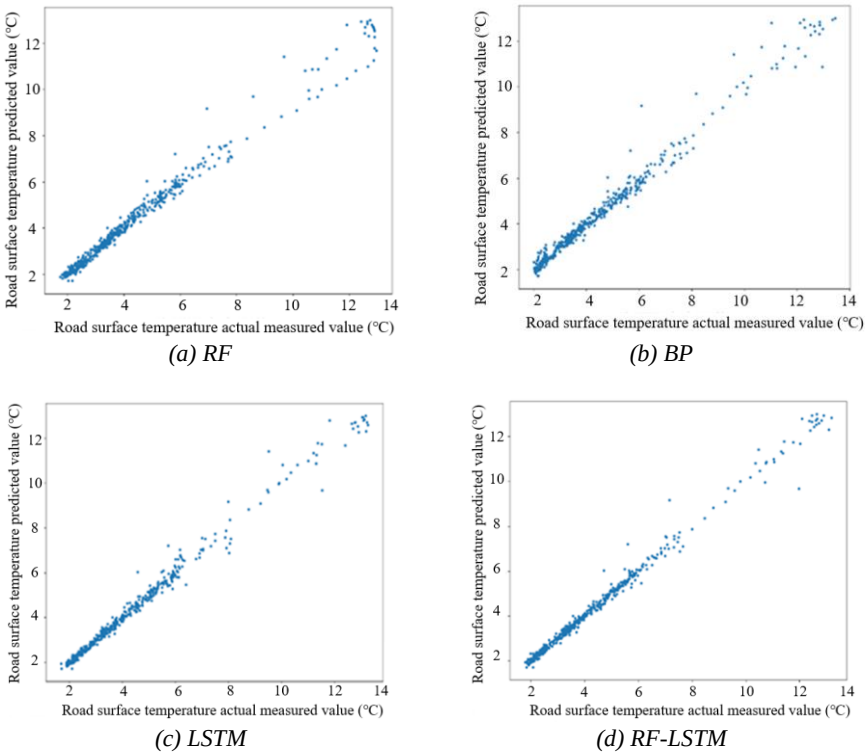

Figure 9 – Transferability of different models

5. CONCLUSIONS

Highways are evolving swiftly from being merely information-based to becoming fully intelligent, with smart highways, vehicle-road coordination and intelligent network interconnection emerging as key directions for the next generation of intelligent transportation systems (ITS). As intelligent highway control technologies and their demands grow, ensuring safe driving under adverse weather conditions through intelligent network interconnection or vehicle-road coordination has been acknowledged globally as a significant challenge, requiring more immediate low-temperature icing warnings, shifting from hourly-level to minute-level notifications. This study proposes a data-driven method for predicting road surface temperature (RST) during winter in mountain areas, leveraging both feature selection and deep learning techniques. The method employs random forest (RF) to extract crucial environmental feature variables affecting RST from raw meteorological data in Yunnan, China. By testing different combinations of feature variables, the optimal input variable combination was determined and integrated into a long short-term memory (LSTM) model to construct the short-term RF-LSTM model for RST prediction. The RF module identified five crucial feature variables that play a significant role in shaping RST: temperature, air pressure, wind speed, humidity and wind direction. The most effective input combination for the RST prediction was found to be RST and temperature. RST is mainly affected by the short-term and long-term memory features of input features within two hours.

The RF-LSTM model exhibited high prediction accuracy with an average absolute error of 0.184°C and an impressive prediction accuracy of 99.13% within the allowable error margin of ±0.5°C, which is superior to the baseline models (the RF model, the BP model and the standard LSTM model). By refining input variable combinations and fine-tuning model parameters, the model's complexity was reduced and the abrupt noise signals were eliminated, preventing model overfitting. Updating the LSTM model parameters through short-term and long-term memory features in real-time also helps reduce RST prediction errors, making this model practical.

The RF-LSTM model was tested for model transferability using a validation dataset. While there was a slight increase in prediction error, the RF-LSTM model, which combines RF feature selection and short-term and long-term memory features, was significantly superior to conventional machine learning models, especially in the low-temperature range (0~2.5℃) during winter. The model demonstrated good generalisation performance.

The accurate prediction of winter highway pavement temperature and the early detection of road icing risks are crucial for enhancing road maintenance efficiency and traffic safety. This significance is underscored by the highway winter management practices, as evidenced by the literature [25-28]. The evaluation of the impact of short-term road surface temperature prediction and icing warnings on road safety is another important research area, requiring extensive data collection both before and after the implementation of such systems.

In future work, we plan to collect a more comprehensive and long-term dataset, covering a wider range of mountain road surfaces, a greater variety of meteorological characteristics, as well as various spatio-temporal factors (such as different times, altitudes and architectural environments), to enhance the predictive capability of the RF-LSTM model under high-temperature conditions, as well as its spatio-temporal transferability. The ultimate goal is to harness the prediction model for practical applications in the winter road icing short-term warning and service systems and assess the safety and mobility effect of early warning of RST and road icing in these systems.

ACKNOWLEDGMENT

This work was jointly supported by the National Key Research and Development Program of China (2019YFB1600100), the Science and Technology Innovation Program of the Department of Transportation, Yunnan Province (No. 2023-83-01) and the Science and Technology Program of Yunnan Science Research Institute of Communication Co., Ltd (No. JKYZLX-2023-12).

REFERENCES

[1] Theofilatos A, Yannis G. A review of the effect of traffic and weather characteristics on road safety. *Accident Analysis & Prevention*. 2014;72:244–256. DOI: 10.1016/j.aap.2014.06.017.

[2] Li Y, et al. Probability prediction of pavement surface low temperature in winter based on Bayesian structural time series and neural network. *Cold Regions Science and Technology*. 2022;194:103434. DOI: 10.1016/j.coldregions.2021.103434.

[3] Sukuvaara T, et al. ITS-Enabled advanced road weather services and infrastructures for vehicle winter testing, professional traffic fleets and future automated driving. In *Proceedings of the 2018 ITS World Congress*, Copenhagen, Denmark. 2018;17–21.

[4] Crevier L, Delage Y. METRo: A new model for road-condition forecasting in Canada. *Journal of Applied Meteorology and Climatology*. 2001;40(11):2026–2037. DOI: 10.1175/1520-0450(2001)040.

[5] Coudert O, et al. Optima (Road weather information dedicated to road sections). In *Proc. 16th Int. Road Weather Conf.* 2012;1–7.

[6] Kangas M, et al. RoadSurf: A modelling system for predicting road weather and road surface conditions. *Meteorological Applications*. 2015;22(3):544–553. DOI: 10.1002/met.1486.

[7] Kršmanc R, et al. Upgraded METRo model within the METRoSTAT project. In *Proc. of the 17th SIRWEC Conference*. 2014;30:1–8.

[8] Karsisto V, et al. Comparing the performance of two road weather models in the Netherlands. *Weather and Forecasting*. 2017;32(3):991–1006. DOI: 10.1175/WAF-D-16-0158.1.

[9] Sokol Z, et al. Ensemble forecasts of road surface temperatures. *Atmospheric Research*. 2017;187:33–41. DOI: 10.1016/j.atmosres.2016.12.010.

[10] Yin Z, et al. On statistical nowcasting of road surface temperature. *Meteorological Applications*. 2019;26(1):1–13. DOI: 10.1002/met.1729.

[11] Kršmanc R, et al. Statistical approach for forecasting road surface temperature. *Meteorological Applications*. 2013;20(4):439–446. DOI: 10.1002/met.1305.

[12] Tang J, et al. Pavement temperature short impending prediction based on ARIMA in winter. *Journal of Tongji University (Natural Science)*. 2017;45(12):1824–1829. DOI: 10.11908/j.issn.0253-374x.2017.12.012.

[13] Xu B, et al. Temperature prediction model of asphalt pavement in cold regions based on an improved BP neural network. *Applied Thermal Engineering*. 2017;120:568–580. DOI: 10.1016/j.applthermaleng.2017.04.024.

[14] Liu B, et al. Road surface temperature prediction based on gradient extreme learning machine boosting. *Computers in Industry*, 2018;99:294–302. DOI: 10.1016/j.compind.2018.03.026.

[15] Wang K, et al. Forecasts of road surface temperature in winter based on random forests regression. *Meteorological Monthly*. 2021;47(1):82–93. DOI: 10.7519/j.issn.1000-0526.2021.01.008.

[16] Qiu X, et al. Prediction of temperature of asphalt pavement surface based on APRIORI-GBDT Algorithm. *Journal of Highway and Transportation Research and Development*. 2019;36:1–10. DOI: 10.1061/9780784483183.020.

[17] Hochreiter S, Schmidhuber, J. Long short-term memory. *Neural Computation*. 1997;9(8):1735–1780. DOI: 10.1162/neco.1997.9.8.1735.

[18] Chen X, et al. A safety control method of car-following trajectory planning based on LSTM. *Promet-Traffic&Transportation*. 2023;35(3):380–394. DOI: 10.7307/ptt.v35i3.118.

[19] Jiang R, et al. Predicting bus travel time with hybrid incomplete data–a deep learning approach. *Promet-Traffic&Transportation*. 2022;34(5):673–685. DOI: 10.7307/ptt.v34i5.4052.

[20] Tabrizi S, et al. Hourly road pavement surface temperature forecasting using deep learning models. *Journal of Hydrology*. 2021;603:126877. DOI: 10.1016/j.jhydrol.2021.126877.

[21] Dai B, et al. Hourly road surface temperature LSTM prediction model of expressway in winter. *China Safety Science Journal*. 2023;33(1):136. DOI: 10.16265/j.cnki.issn1003-3033.2023.01.2215.

[22] Breiman L. Random forests. *Machine learning*. 2021;45:5–32. DOI: 10.1023/A:1010933404324.

[23] Li H, Guo Y. Estimating factors influencing the capacity of the wide-road-and-narrow-bridge section based on random forest. *Promet-Traffic&Transportation*. 2023;35(1):1–11. DOI: 10.7307/ptt.v35i1.46.

[24] Hecht-Nielsen R. Theory of the backpropagation neural network. In Neural networks for perception. *Academic Press*, 1992;65–93.

[25] Gregurić M, et al. Towards the spatial analysis of motorway safety in the connected environment by using explainable deep learning. *Knowledge-Based Systems*. 2023;269:110523. DOI: 10.1016/j.knosys.2023.110523.

[26] Theofilatos A, Yannis G. A review of the effect of traffic and weather characteristics on road safety. *Accident Analysis & Prevention*. 2014;72:244–256. DOI: 10.1016/j.aap.2014.06.017.

[27] Dey K, et al. Potential of intelligent transportation systems in mitigating adverse weather impacts on road mobility: A review. *IEEE Transactions on Intelligent Transportation Systems*. 2015;16(3):1107–1119. DOI: 10.1109/TITS.2014.2371455.

[28] Songchitruksa P, Balke K. Assessing weather, environment, and loop data for real-time freeway incident prediction. *Journal of Transportation Research Record*. 2006;1959:105–113. DOI: 10.1177/0361198106195900112.

张孟, 郭华, 李京阳, 李立, 朱峰

高海拔山区冬季路表温度实时预测的深度学习方法

摘要

冬季低温结冰是严重影响公路安全和交通运行的重要因素。为了提高高原山区公路冬季路表温度(简称：RST)实时预测的准确性和可靠性，构建了一种基于特征选择和深度学习的路表温度短时预测模型。利用中国云南某山区高速公路的气象观测数据，首先采用随机森林（random forests，RF）模型提取影响路表温度的重要环境特征变量，并根据重要特征参数与路表温度的排序组合，优化深度学习预测模型的多维输入；其次，以 10min 为更新频率，使用长短时记忆神经网络（long short-term memory，LSTM）构建冬季路表温度短时预测模型（简称：RF-LSTM），通过对比实验确定预测模型的最佳输入变量组合和预设参数；最后，与常见机器学习模型进行比较，分析路表温度预测的精度，并验证预测模型的可移植性。结果表明：RF-LTSM 路表温度短时预测模型的最佳输入变量组合是路表温度和气温；短时路表温度受 2 小时内长短时记忆特征的影响；模型的预测平均绝对误差比 RF 模型、BP（back propagation）神经网络模型和 LSTM 模型分别下降 59.15%、31.10%和 20.26%，且在±0.5℃允许误差范围内的预测准确率为 99.13%；在验证数据集上模型

预测平均绝对误差为 0.0478，具有较好的时间可移植性。整体而言，所提出的模型实现了实时 RST 的高精度预测，且在高海拔和山区的复杂条件下，模型的预测性能稳定可靠，可为交通安全和道路维护提供了更有力的决策支持。

关键词：
智能交通系统；路表温度预测；长短时记忆模型；特征变量组合；可移植性；山区公路